Ca^{2+} cycling properties are conserved despite bradycardic effects of heart failure in sinoatrial node cells

Arie O. Verkerk[1]*, Marcel M. G. J. van Borren[1,2], Antoni C. G. van Ginneken[1] and Ronald Wilders[1]

[1] Department of Anatomy, Embryology and Physiology, Academic Medical Center, University of Amsterdam, Amsterdam, Netherlands
[2] Laboratory of Clinical Chemistry and Haematology, Rijnstate Hospital, Arnhem, Netherlands

Background: In animal models of heart failure (HF), heart rate decreases due to an increase in intrinsic cycle length (CL) of the sinoatrial node (SAN). Pacemaker activity of SAN cells is complex and modulated by the membrane clock, i.e., the ensemble of voltage gated ion channels and electrogenic pumps and exchangers, and the Ca^{2+} clock, i.e., the ensemble of intracellular Ca^{2+} ($[Ca^{2+}]_i$) dependent processes. HF in SAN cells results in remodeling of the membrane clock, but few studies have examined its effects on $[Ca^{2+}]_i$ homeostasis.

Methods: SAN cells were isolated from control rabbits and rabbits with volume and pressure overload-induced HF. $[Ca^{2+}]_i$ concentrations, and action potentials (APs) and Na^+-Ca^{2+} exchange current (I_{NCX}) were measured using indo-1 and patch-clamp methodology, respectively.

Results: The frequency of spontaneous $[Ca^{2+}]_i$ transients was significantly lower in HF SAN cells (3.0 ± 0.1 ($n = 40$) vs. 3.4 ± 0.1 Hz ($n = 45$); mean ± SEM), indicating that intrinsic CL was prolonged. HF slowed the $[Ca^{2+}]_i$ transient decay, which could be explained by the slower frequency and reduced sarcoplasmic reticulum (SR) dependent rate of Ca^{2+} uptake. Other $[Ca^{2+}]_i$ transient parameters, SR Ca^{2+} content, I_{NCX} density, and I_{NCX}-$[Ca^{2+}]_i$ relationship were all unaffected by HF. Combined AP and $[Ca^{2+}]_i$ recordings demonstrated that the slower $[Ca^{2+}]_i$ transient decay in HF SAN cells may result in increased I_{NCX} during the diastolic depolarization, but that this effect is likely counteracted by the HF-induced increase in intracellular Na^+. β-adrenergic and muscarinic stimulation were not changed in HF SAN cells, except that late diastolic $[Ca^{2+}]_i$ rise, a prominent feature of the Ca^{2+} clock, is lower during β-adrenergic stimulation.

Conclusions: HF SAN cells have a slower $[Ca^{2+}]_i$ transient decay with limited effects on pacemaker activity. Reduced late diastolic $[Ca^{2+}]_i$ rise during β-adrenergic stimulation may contribute to an impaired increase in intrinsic frequency in HF SAN cells.

Keywords: heart failure, pacemaker activity, intracellular Ca^{2+}, Ca^{2+} clock, membrane clock, sinoatrial node, action potentials, sodium-calcium exchanger

INTRODUCTION

Pacemaker activity of the sinoatrial node (SAN) is controlled by a complex system of clocks composed of time- and voltage-dependent sarcolemmal currents, designated the voltage or membrane clock (Mangoni and Nargeot, 2008), and tightly coupled sarcoplasmic reticulum (SR) Ca^{2+} cycling molecules together with the Na^+-Ca^{2+} exchange current (I_{NCX}), named the Ca^{2+} clock (Lakatta et al., 2010). The primary mechanism of SAN pacemaking is heavily debated (DiFrancesco and Robinson, 2002; Kodama et al., 2002; Vinogradova et al., 2002b; Honjo et al., 2003; Lakatta et al., 2003; Lipsius and Bers, 2003; Bers, 2006a; Lakatta and DiFrancesco, 2009; DiFrancesco, 2010; Maltsev and Lakatta, 2010a, 2012; Verkerk and Wilders, 2010; Himeno et al., 2011a,b; Maltsev et al., 2011; DiFrancesco and Noble, 2012a,b; Lakatta and Maltsev, 2012), but it likely involves a tight collaboration of

both clock systems, because intracellular Ca^{2+} ($[Ca^{2+}]_i$) affects various membrane currents directly, e.g., I_{NCX} (Blaustein and Lederer, 1999), hyperpolarization-activated current (I_f) (Rigg et al., 2003), slow component of delayed rectifier K^+ current (I_{Ks}) (Tohse, 1990), long lasting Ca^{2+} current ($I_{Ca,L}$) (Sipido et al., 1995), transient Ca^{2+} current ($I_{Ca,T}$) (Lacinová et al., 2006), Cl^- current (Arai et al., 1996; Verkerk et al., 2002), and/or indirectly via calmodulin-dependent protein kinase II (CaMKII) (Wu and Anderson, 2014), and changes in membrane current affect pacemaker rate with resultant changes in $[Ca^{2+}]_i$ (Lakatta et al., 2010; van Borren et al., 2010).

Heart failure (HF) reduces pacemaker activity of SAN cells through an increase in intrinsic cycle length (Opthof et al., 2000; Witte et al., 2000; Verkerk et al., 2003; Du et al., 2007). Previously, it has been shown that this was al least due to

remodeling of components of the membrane clock. HF impairs the membrane clock by downregulation of I_f in the SAN of rabbit (Verkerk et al., 2003) and downregulation of the corresponding hyperpolarization-activated (HCN) channel subunits, HCN4 and HCN2, in the SAN of dogs (Zicha et al., 2005). In addition, TTX-sensitive neuronal Na^+ channels, $Na_v1.1$ and $Na_v1.6$, are downregulated in SAN tissue of HF rats (Du et al., 2007). Finally, HF upregulates I_{Ks} in HF SAN cells of rabbit (Verkerk et al., 2003), but since I_{Ks} plays a limited role in pacemaker activity without adrenergic stimulation (Lei et al., 2000), this change in membrane clock is hardly involved in the increase in intrinsic cycle length during HF (Verkerk et al., 2003).

To date, the effect of HF on $[Ca^{2+}]_i$ homeostasis in atrial and ventricular myocytes has been studied in detail (for reviews, see Bers, 2006b; Bers et al., 2006; Kho et al., 2012; Eisner et al., 2013; Luo and Anderson, 2013; Neef and Maier, 2013), but the effect of HF on $[Ca^{2+}]_i$ in SAN cells is hardly known. Shinohara et al. (2010) found that HF, induced by rapid ventricular pacing, results in Ca^{2+} clock malfunction in SAN of dogs, characterized by a reduction of the slope of late diastolic Ca^{2+} elevation (LDCAE) as well as unresponsiveness to isoproterenol and caffeine in intact SAN. Especially the reduced slope of the LDCAE, with associated decrease in localized Ca^{2+} releases (LCRs) or Ca^{2+} sparks (Bogdanov et al., 2006; Maltsev et al., 2006; Joung et al., 2009, 2010; van Borren et al., 2010), may have implications for the Ca^{2+} clock (Stern et al., 2014).

In the present study, we evaluated the $[Ca^{2+}]_i$ homeostasis in isolated control (CTRL) and HF SAN cells using a well-established rabbit model of volume and pressure overload-induced HF. We found a slower spontaneous $[Ca^{2+}]_i$ transient frequency in HF SAN cells, indicating that the intrinsic cycle length was prolonged. HF slowed the $[Ca^{2+}]_i$ transient decay without changes in diastolic and systolic $[Ca^{2+}]_i$ concentrations, LDCAE, and SR Ca^{2+} content. The reduced $[Ca^{2+}]_i$ transient decay velocity was partially, but not completely, explained by the slower intrinsic frequency of HF SAN cells. Neither the I_{NCX} density nor the I_{NCX}-$[Ca^{2+}]_i$ relationship were affected by HF. Combined action potential and $[Ca^{2+}]_i$ measurements demonstrated that the decreased $[Ca^{2+}]_i$ transient decay velocity has limited effect on I_{NCX} during diastolic depolarization.

MATERIALS AND METHODS

CELL PREPARATION

The investigation was approved by the local ethics committee and conformed to the guiding principles of the *Declaration of Helsinki*. HF was induced in 5-month-old male New-Zealand White rabbits by combined volume- and pressure-overload in 2 sequential surgical procedures as described previously (Vermeulen et al., 1994; Verkerk et al., 2011). In short, volume overload was produced by rupture of the aortic valve until pulse pressure was increased by about 60–90%. Three weeks later, pressure overload was created by suprarenal abdominal aorta constriction of approximately 50%. Four months after the last operation, the rabbits were anaesthetized [ketamine (50 mg im; Eurovet, Bladel, The Netherlands) and xylazine (10 mg im; Eurovet, Bladel, The Netherlands)], heparinized (5000 IU, LEO Pharma, Breda, The Netherlands), and killed by intravenous injection of pentobarbital (240 mg; Ceva

Sante Animale B.V., Maassluis, The Netherlands). Relative heart weight (i.e., heart weight to body weight ratio), relative lung weight (i.e., lung weight to body weight ratio), and presence of ascites were analyzed as described previously (Vermeulen et al., 1994). Sham-operated rabbits undergoing thoracotomy and age-matched non-operated rabbits do not differ in various heart failure parameters (Vermeulen et al., 1994) and important cellular parameters for hypertrophy and ionic remodeling (Verkerk et al., 2011). In the present study, therefore, non-operated age-matched healthy animals served as control (CTRL). A total of 12 HF and 13 CTRL rabbits were used.

Single SAN cells were enzymatically isolated from the entire SAN region as described previously (Verkerk et al., 2009). Small aliquots of cell suspension were put in a recording chamber on the stage of an inverted microscope. Cells were allowed to adhere for 5 min after which superfusion with Tyrode's solution was started. Tyrode's solution ($36 \pm 0.2°C$) contained (in mM): NaCl 140, KCl 5.4, $CaCl_2$ 1.8, $MgCl_2$ 1.0, glucose 5.5, HEPES 5.0, pH 7.4 (NaOH). Spindle and elongated spindle-like cells displaying regular contractions were selected for measurements.

CALCIUM MEASUREMENTS

$[Ca^{2+}]_i$ was measured in spontaneously active indo-1 (Molecular Probes, Eugene, OR, USA) loaded myocytes as described previously in detail (van Borren et al., 2010). Such signals are a measure of global $[Ca^{2+}]_i$ transients, which are triggered by Ca^{2+} influx through sarcolemmal Ca^{2+} channels activated during spontaneous action potentials. As indicated in the Introduction section, these spontaneous action potentials in SAN cells likely involve a tight collaboration of both membrane and Ca^{2+} clock systems. Of note, in this study we used the term "spontaneous $[Ca^{2+}]_i$ transient" analog to "spontaneous action potentials," without assumptions regarding the primary cause of the spontaneous activity. As before, we discerned and analyzed five distinct phases in $[Ca^{2+}]_i$ transients of SAN cells (van Borren et al., 2010): (1) minimum diastolic $[Ca^{2+}]_i$ concentration, (2) maximum systolic $[Ca^{2+}]_i$ concentration, (3) maximum rate of the fast systolic $[Ca^{2+}]_i$ rise, (4) time constant of monoexponential $[Ca^{2+}]_i$ transient decay, and (5) mean rate of the slow diastolic $[Ca^{2+}]_i$ rise during the final third of diastolic depolarization until the fast systolic $[Ca^{2+}]_i$ transient. Ten consecutive spontaneous $[Ca^{2+}]_i$ transients were used to determine the average parameters. To date, SR Ca^{2+} content and the rate of Ca^{2+} uptake into the SR by sarco/endoplasmic reticulum Ca^{2+}-ATPase (SERCA) in cardiac working myocytes are frequently measured using caffeine-induced $[Ca^{2+}]_i$ transients combined with simultaneous I_{NCX} recordings with the patch clamp methodology (Varro et al., 1993), which also allows specific pre-pacing protocols. In SAN cells, however, we were unable to measure reliably the I_{NCX} during caffeine-induced Ca^{2+} transients, due to cell membrane rupture resulting in large "leak" currents in response to the strong and fast caffeine-induced contractions. Therefore, we assessed SR Ca^{2+} content as the fractional release of SR Ca^{2+} (Bers, 1987; Bassani et al., 1992) by comparing the amplitude of the spontaneous $[Ca^{2+}]_i$ transients (average of the preceding six successive spontaneous $[Ca^{2+}]_i$ transients) with that of 20 mM caffeine-evoked $[Ca^{2+}]_i$ transient in the presence of 5 mM $NiCl_2$, to block the

I$_{NCX}$. The rate of decay was obtained by fitting single exponential functions to the decay phase of the caffeine-evoked [Ca^{2+}]$_i$ transients.

ELECTROPHYSIOLOGY

Action potentials and I$_{NCX}$ were recorded by the amphotericin-perforated patch-clamp technique using an Axopatch 200B amplifier (Molecular Devices, USA). Patch pipettes (borosilicate glass, 2–5 MΩ) were filled with solution containing (in mM): K-gluc 120, KCl 20, NaCl 5, amphotericin-B 0.22, NMDG-Cl (N-methyl-D-glucammonium chloride) 10, HEPES 10, pH 7.2 (KOH 5.5). Series resistance was compensated by ≥80%, and potentials were corrected for the calculated liquid junction potential. Action potentials were low-pass filtered (cut-off frequency: 1 kHz) and digitized at 1 kHz; I$_{NCX}$ was filtered and digitized at 1 and 0.2 kHz, respectively. Voltage control and data acquisition were accomplished using pCLAMP 8 software (Molecular Devices, USA), while custom software was used for data analysis. Cell membrane capacitance was estimated by dividing the time constant of the decay of the capacitive transient in response to 5 mV hyperpolarizing voltage clamp steps from 0 mV by the series resistance, and amounted to 50.0 ± 6.9 pF in CTRL ($n = 5$) and 56.1 ± 8.1 pF in HF ($n = 5$) SAN cells (mean ± SEM, $P > 0.05$), in line with the values of 50 ± 4 ($n = 23$) and 52 ± 3 pF ($n = 24$) that we observed in a previous study (Verkerk et al., 2003). I$_{NCX}$ density and the I$_{NCX}$-[Ca^{2+}]$_i$ relationship were measured as described previously (Weber et al., 2003). In short, a slow depolarizing voltage ramp from −85 to 120 mV results in an increase in [Ca^{2+}]$_i$ due to Ca^{2+} entry through NCX operating in reverse mode (net outward I$_{NCX}$). Upon fast repolarization, Ca^{2+} removal occurs resulting in a [Ca^{2+}]$_i$ decline due to Ca^{2+} efflux through NCX operating in forward mode (net inward I$_{NCX}$) (Weber et al., 2003). The relationship between [Ca^{2+}]$_i$ and I$_{NCX}$ is membrane potential dependent, with a steeper relationship at more negative membrane potentials (Hove-Madsen and Tort, 2001). We used a repolarizing potential of −60 mV, which is close to the maximal diastolic potential of both CTRL and HF SAN cells (Verkerk et al., 2003). Thapsigargin (2.5 μM) was added to the Tyrode's solution to block SERCA. In addition, chromanol (5 μM) and E4031 (5 μM) were present to block the slow and rapid components of the delayed rectifier K$^+$ current, while CsCl (5 mM) was present to block I$_f$. All drugs were obtained from Sigma (Zwijndrecht, The Netherlands) except for E4031, which was a gift from Eisai (Tokyo, Japan), and noradrenaline (Centrafarm, Etten-Leur, The Netherlands). I$_{NCX}$ densities were calculated by dividing current amplitudes by the cell membrane capacitance.

NUMERICAL RECONSTRUCTION OF SODIUM-CALCIUM EXCHANGE CURRENT

For the numerical reconstruction of I$_{NCX}$ on the basis of the simultaneously recorded experimental data on the membrane potential (V$_m$) and [Ca^{2+}]$_i$ (combined voltage and calcium clamp, van Borren et al., 2007), we adopted the I$_{NCX}$ formulation of the Lindblad et al. model for a rabbit atrial myocyte (Lindblad et al., 1996), with I$_{NCX}$ scaled down to 78% of its control value, based on mRNA data from Allah et al. (2011). We thus followed the approach of our previous study in which we reconstructed

rabbit SAN I$_{NCX}$ in order to compare it with human SAN I$_{NCX}$ (Verkerk et al., 2013).

The Lindblad et al. (1996) equations not only require values for V$_m$ and [Ca^{2+}]$_i$, but also for [Ca^{2+}]$_e$, [Na$^+$]$_e$ and [Na$^+$]$_i$, which denote the extracellular Ca^{2+} concentration, the extracellular Na$^+$ concentration, and the intracellular Na$^+$ concentration, respectively. [Ca^{2+}]$_e$ and [Na$^+$]$_e$ were set to 1.8 and 140 mM, respectively, in accordance with the aforementioned Tyrode's solution, whereas [Na$^+$]$_i$ was set to 5 mM, based on the pipette solution. In some reconstructions, [Na$^+$]$_i$ was raised to 7.5 mM, as indicated.

STATISTICS

Data are mean ± SEM. Groups of HF SAN cells were compared with groups of CTRL SAN cells using Fisher's exact test, Two-Way Repeated Measures ANOVA followed by pairwise comparison using the Student-Newman-Keuls test, and unpaired t-test. Paired t-tests were used to compare drug effects within a group. An F-test was used to compare frequency dependency between groups. $P < 0.05$ is considered statistically significant.

RESULTS

HF MODEL CHARACTERISTICS

Table 1 summarizes the general characteristics of the HF model. Consistent with previous reports of the volume- and pressure-overload rabbit model of HF (Vermeulen et al., 1994; Baartscheer et al., 2003a,b; Verkerk et al., 2003, 2011; Wiegerinck et al., 2006) body weight was similar, but heart weight was significantly higher in HF compared to CTRL rabbits. Consequently relative heart weight was significantly higher in HF rabbits. In addition, HF rabbits had an increased lung weight and relative lung weight. Moreover, six out of the 12 HF rabbits used in the present study exhibited ascites as assessed during autopsy, while none of the 13 CTRL rabbits did. Finally, we measured the weight of the right atrium to determine whether HF affects also the right atrium including the SAN. We found that both the absolute weight of the right atrium and the relative right atrial weight were significantly higher in HF rabbits.

HF REDUCES THE FREQUENCY AND Ca^{2+} TRANSIENT DECAY OF SAN CELLS

Figure 1A shows typical recordings of [Ca^{2+}]$_i$ transients from SAN cells of a CTRL and a HF rabbit; Figure 1B summarizes the

Table 1 | Characteristics of the control (CTRL) and heart failure (HF) model.

	CTRL (N = 13)	HF (N = 12)
Body weight (kg)	3.90 ± 0.09	3.92 ± 0.13
Heart weight (g)	9.0 ± 0.4	19.2 ± 1.3*
Relative heart weight (g kg^{-1})	2.31 ± 0.08	4.90 ± 0.26*
Lung weight (g)	12.2 ± 0.4	18.8 ± 1.3*
Relative lung weight (g kg^{-1})	3.13 ± 0.08	4.84 ± 0.35*
Presence of ascites (%)	0	50*
Right atrium weight (g)	0.37 ± 0.04	0.86 ± 0.16*
Relative right atrium weight (g kg^{-1})	0.09 ± 0.01	0.22 ± 0.04*

*$P < 0.05$ vs. CTRL. N, number of rabbits.

FIGURE 1 | Heart failure (HF) reduces the frequency and intracellular Ca^{2+} ([Ca^{2+}]$_i$) transient decay of sinoatrial (SAN) cells. (A) Representative [Ca^{2+}]$_i$ transients in a SAN cell isolated from a control (CTRL) and HF rabbit. (B) Average [Ca^{2+}]$_i$ transient characteristics. *$P < 0.05$.
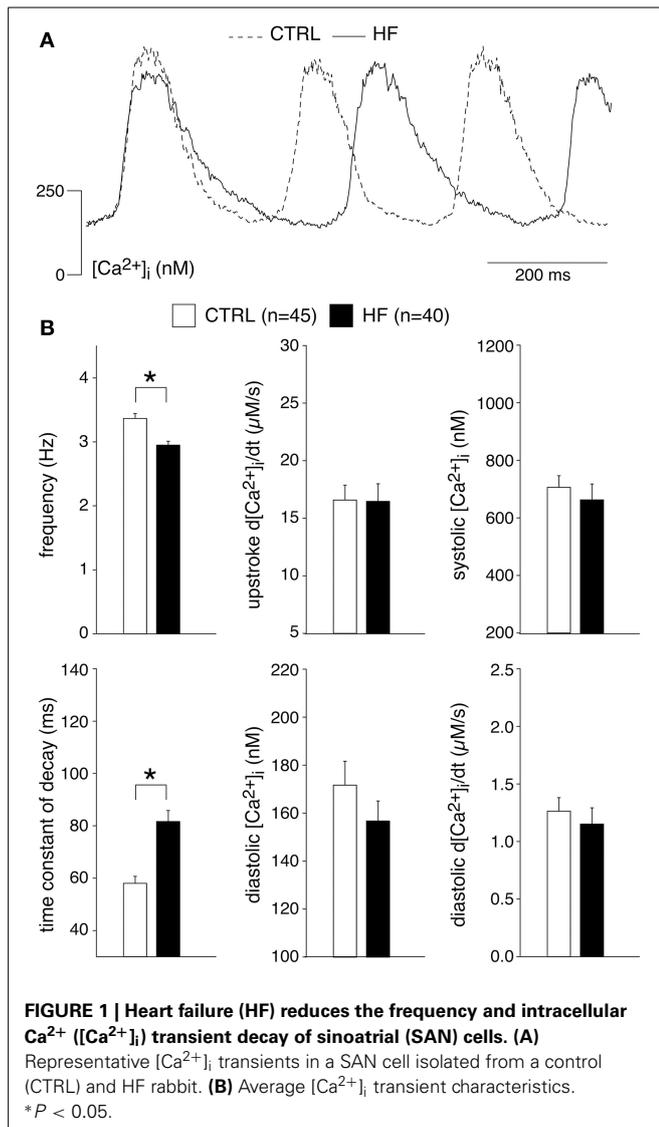
average [Ca^{2+}]$_i$ characteristics. In SAN cells, spontaneous action potentials are accompanied by [Ca^{2+}]$_i$ transients in a 1:1 fashion in CTRL (Li et al., 1997; Rigg et al., 2000; Lakatta et al., 2003; Joung et al., 2009, 2010; van Borren et al., 2010) as well as in HF SAN cells (see **Figure 7**, below). Thus, the rate of spontaneous SAN [Ca^{2+}]$_i$ transients is a measure of the intrinsic beating rate. We found a significantly lower frequency of spontaneous [Ca^{2+}]$_i$ transients in HF SAN cells [**Figure 1B**, top left; 2.95 ± 0.06 (HF) vs. 3.37 ± 0.08 (CTRL) Hz], indicating that intrinsic cycle length was prolonged in HF SAN cells. The upstroke velocity of the [Ca^{2+}]$_i$ transient and the systolic [Ca^{2+}]$_i$ transient concentration were not significantly different in HF SAN cells compared with CTRL SAN cells (**Figure 1B**, top right panels). The decay of the [Ca^{2+}]$_i$ transient was significantly slowed in HF SAN cells, as indicated by the significant increase in the time constant of decay (**Figure 1B**, bottom left). On average, [Ca^{2+}]$_i$ transient time constant of decay [81.6 ± 4.2 (HF) vs. 57.8 ± 2.6 (CTRL) ms] is ≈41% larger than in CTRL SAN cells. Neither

the diastolic [Ca^{2+}]$_i$ concentration nor the late diastolic [Ca^{2+}]$_i$ rise (diastolic d[Ca^{2+}]$_i$/dt) were significantly different in HF SAN cells compared with CTRL SAN cells (**Figure 1B**, bottom right panels).

In ventricular myocytes, [Ca^{2+}]$_i$ transient parameters are action potential duration (Weber et al., 2003) and frequency-dependent (Hussain et al., 1997; Dibb et al., 2007), while in the SAN an increase in late diastolic [Ca^{2+}]$_i$ rise was observed at higher beating rates (Joung et al., 2009). The role of the action potential duration in the observed slower [Ca^{2+}]$_i$ transient decay is likely limited, because the action potential duration in CTRL and HF SAN cells is similar (Verkerk et al., 2003). However, the decay of the [Ca^{2+}]$_i$ transient has a strong frequency dependency with a slower decay at slower frequencies (Hussain et al., 1997; Dibb et al., 2007). Thus, the slower [Ca^{2+}]$_i$ transient decay that we observed in HF SAN cells may be related to its slower intrinsic frequency. To test this hypothesis, we determined the relationship between frequency and [Ca^{2+}]$_i$ properties by plotting each of the five [Ca^{2+}]$_i$ transient parameters of every cell against its own frequency. The data have been fitted with linear regression lines (**Figure 2**). The linear fits to the CTRL as well as HF SAN cell data have all slopes significantly different from zero (see **Table 2**). However, neither the slopes nor the intercepts are significantly different between CTRL and HF for each of the five parameters (**Table 2**). Thus, while there are clear relationships between all five [Ca^{2+}]$_i$ transient parameters and frequency, these relationships do not differ significantly between CTRL and HF SAN cells. The ≈41% difference in [Ca^{2+}]$_i$ transient time constant of decay between HF and CTRL cells (**Figure 1B**) is larger than expected from the linear regression of the [Ca^{2+}]$_i$ transient time constant of decay vs. frequency relationship. Using the slope and intercept of the regression line for all cells, which amount to 151 (intercept) and −26 (slope), respectively, the difference in frequency between HF and CTRL cells explains only a ≈17% difference.

From these data we conclude that HF reduces the frequency and slows the Ca^{2+} transient decay of SAN cells, the latter partially explained by the slower frequency in HF SAN cells.

HF DOES NOT AFFECT THE SR Ca^{2+} CONTENT OF SAN CELLS

Our experiments demonstrate a reduced [Ca^{2+}]$_i$ transient decay rate, partially explained by a slower intrinsic frequency. The decline of the [Ca^{2+}]$_i$ transient is mainly due to uptake into the SR through SERCA and extrusion of Ca^{2+} via the sarcolemmal Na$^+$–Ca^{2+} exchange (NCX), while mitochondrial Ca^{2+} uptake and sarcolemmal Ca-ATPase may contribute for a very small fraction (Bers, 2006b; Dibb et al., 2007). In ventricular myocytes, a slower decline of the [Ca^{2+}]$_i$ transient by downregulation of SERCA results in a reduced SR Ca^{2+} content (Bers, 2006b; Bers et al., 2006), while a slower decline of the [Ca^{2+}]$_i$ transient due to downregulation of the NCX may result in increased SR Ca^{2+} content (Bers, 2006b; Eisner et al., 2013). To gain insight into the relationship in SAN cells, we analyzed the amplitude of the normal spontaneous [Ca^{2+}]$_i$ transient as a fraction of the caffeine-evoked transient in the presence of 5 mM NiCl$_2$, termed fractional release, which is an estimate of the proportion of the SR Ca^{2+} content released during each spontaneous transient. **Figure 3A** shows typical recordings in SAN cells from a CTRL

FIGURE 2 | The relationships between frequency and $[Ca^{2+}]_i$ transient parameters are not affected by HF. (A) Typical $[Ca^{2+}]_i$ transients of a fast (solid line) and slow (dashed line) beating CTRL and HF SAN cell.

(B) Scatter plot of $[Ca^{2+}]_i$ transient parameters of all cells measured vs. frequency. Solid and dashed lines: linear fits to HF and CTRL data, respectively.
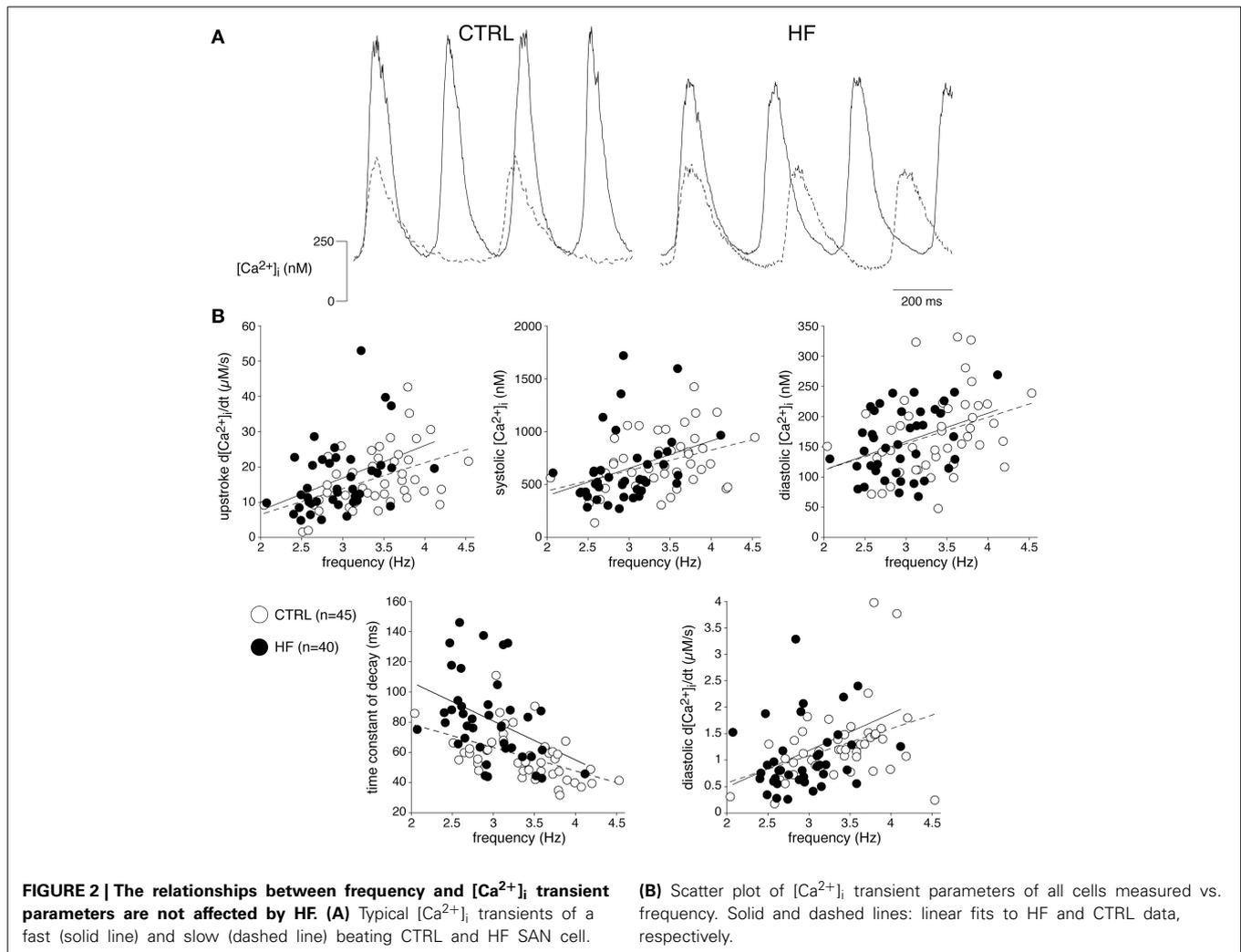
Table 2 | Frequency-dependency of $[Ca^{2+}]_i$ transient parameters in CTRL and HF SAN cells.

	CTRL ($n = 45$)		HF ($n = 40$)	
	Slope	Intercept	Slope	Intercept
Upstroke d$[Ca^{2+}]_i$/dt	7.3 ± 2.2	-8.1 ± 7.5	9.2 ± 3.6	-10.7 ± 10.6
Systolic $[Ca^{2+}]_i$	194 ± 73	55 ± 250	260 ± 121	-124 ± 359
Time constant of decay	-16 ± 4	110 ± 14	-26 ± 10	158 ± 29
Diastolic $[Ca^{2+}]_i$	44 ± 18	25 ± 62	47 ± 20	18 ± 59
Diastolic d$[Ca^{2+}]_i$/dt	0.51 ± 0.19	-0.45 ± 0.66	0.70 ± 0.34	-0.90 ± 1.0

Regression lines as in **Figure 2**. *Slope and intercept data are* ± *standard error. All slopes are significantly different from zero.*

and a HF rabbit. The averaged fractional release of CTRL and HF SAN cells did not differ significantly [0.23 ± 0.04 ($n = 23$) vs. 0.22 ± 0.03 ($n = 18$)] (**Figure 3B**). The caffeine-evoked transient in the presence of $NiCl_2$ can also be used to determine

the aforementioned contribution of mitochondrial Ca^{2+} uptake and sarcolemmal Ca-ATPase, because SERCA and NCX function is effectively by-passed by caffeine and Ni^{2+}, respectively (Díaz et al., 2004). The time constant of decay of the caffeine-evoked $[Ca^{2+}]_i$ transient in the presence of 5 mM $NiCl_2$ was 3728 ± 474 (CTRL, $n = 23$) vs. 3654 ± 406 ms (HF, $n = 18$) (**Figure 3C**), indicating that mitochondrial Ca^{2+} uptake and sarcolemmal Ca-ATPase were not affected in HF SAN cells compared to CTRL SAN cells. The relative contribution of the mitochondrial Ca^{2+} uptake and sarcolemmal Ca-ATPase in Ca^{2+} removal was calculated by the use of the time constants of decay of the systolic $[Ca^{2+}]_i$ transient (**Figure 3C**, left) and those of caffeine-evoked $[Ca^{2+}]_i$ transient in the presence of Ni^{2+} (**Figure 3C**, middle) (Díaz et al., 2004). The percentage that mitochondrial Ca^{2+} uptake and sarcolemmal Ca-ATPase contribute to the $[Ca^{2+}]_i$ transient decay was 2.1 ± 0.3 and 2.6 ± 0.4 in CTRL and HF SAN cells, respectively (**Figure 3C**, right).

From these data we conclude that HF neither affects the SR Ca^{2+} content nor the mitochondrial Ca^{2+} uptake and sarcolemmal Ca-ATPase activity of SAN cells.

FIGURE 3 | HF does not affect the sarcoplasmic reticulum (SR) Ca^{2+} content of SAN cells. (A) Typical examples of [Ca^{2+}]$_i$ transients induced by application of 20 mM caffeine in the presence of 5 mM NiCl$_2$. **(B)** Average amplitudes of systolic (Syst) and caffeine-induced (Caff) [Ca^{2+}]$_i$ transients (left panel) and the average fractional release (right panel). **(C)** Average time constants of decay of the systolic and caffeine-induced [Ca^{2+}]$_i$ transients (left panels). Right: fractional contribution of mitochondrial Ca^{2+} uptake and sarcolemmal Ca-ATPase to the [Ca^{2+}]$_i$ transient decay. *$P < 0.05$.

HF AFFECTS NEITHER THE I$_{NCX}$ NOR ITS [Ca^{2+}]$_i$ DEPENDENCY

Previously, the I$_{NCX}$ density was found to be similar in CTRL and HF SAN cells of rabbit (Verkerk et al., 2003). These results were obtained by measurements of Ni$^+$-sensitive currents during a descending ramp, while the free [Ca^{2+}]$_i$ was buffered at 150 nM (Verkerk et al., 2003). HF may affect the relationship between [Ca^{2+}]$_i$ and I$_{NCX}$ (Díaz et al., 2004). Therefore, we next determined the relationship between [Ca^{2+}]$_i$ and I$_{NCX}$ as described previously by Weber et al. (2003). **Figures 4A,B**, show the protocol used and typical examples, respectively. A slowly depolarizing voltage ramp from −85 to 120 mV results in an increase in [Ca^{2+}]$_i$ due to Ca^{2+} entry through reverse mode NCX (**Figure 4B**). Upon repolarization to −60 mV, Ca^{2+} removal occurs (forward mode NCX) resulting in a [Ca^{2+}]$_i$ decline (**Figure 4B**, gray lines), which correlates well with the measured I$_{NCX}$ (**Figure 4B**, black lines) (cf. Weber et al., 2003). **Figure 4C** shows the average I$_{NCX}$-[Ca^{2+}]$_i$ relationships obtained during the repolarization-induced [Ca^{2+}]$_i$ decline in CTRL and HF SAN cells. The I$_{NCX}$-[Ca^{2+}]$_i$ relationships are linear in the physiological range. Neither the I$_{NCX}$ density nor the I$_{NCX}$-[Ca^{2+}]$_i$ relationships differ significantly between HF and CTRL SAN cells (**Figure 4C**). In addition, the time constants of both the [Ca^{2+}]$_i$ and I$_{NCX}$ decline during the repolarizing step to −60 mV, another measure of NCX function (Weber et al., 2003), do not differ significantly between CTRL and HF SAN cells (**Figure 4D**).

From these data we conclude that HF does not affect the I$_{NCX}$ density nor the I$_{NCX}$-[Ca^{2+}]$_i$ dependency. In addition, given the unaltered NCX and mitochondrial Ca^{2+} uptake and sarcolemmal Ca-ATPase activity of SAN cells, we conclude that the slower decay of the [Ca^{2+}]$_i$ transient is due to reduced SERCA activity.

HF HARDLY AFFECTS [Ca^{2+}]$_i$ MODULATION BY ACETHYLCHOLINE AND NORADRENALINE

[Ca^{2+}]$_i$ transients in SAN cells are importantly modulated by β-adrenergic (Rigg et al., 2000; Vinogradova et al., 2002a; Joung et al., 2009; van Borren et al., 2010) and muscarinic receptor (van Borren et al., 2010) stimulation. Most importantly, β-adrenergic stimulation increases the frequency and amplitude of [Ca^{2+}]$_i$ transients as well as local Ca^{2+} releases (LCRs) from the SR late during the diastolic depolarization (Vinogradova et al., 2002a; Joung et al., 2009; van Borren et al., 2010). Muscarinic receptor stimulation with acetylcholine decreases the frequency and amplitude of [Ca^{2+}]$_i$ transients and local Ca^{2+} releases from the SR (van Borren et al., 2010). Opthof et al. (2000) reported an increased sensitivity for acetylcholine in intact HF SAN preparations of rabbit, while Shinohara et al. (2010) found that intact SAN preparations of HF dogs were completely unresponsive to isoproterenol. Here, we tested the effects of β-adrenergic and muscarinic receptor stimulation on [Ca^{2+}]$_i$ transient parameters in CTRL and HF SAN cells. β-adrenergic stimulation with 500 nM noradrenaline significantly increased the frequency and the [Ca^{2+}]$_i$ transient parameters in both CTRL and HF SAN cells (**Figure 5**), except the time constant of decay, which was significantly decreased in the HF SAN cells. In presence of noradrenaline HF SAN cells still have a significantly lower frequency and slower decay phase compared to CTRL SAN cells (**Figure 5B**, left), while

FIGURE 4 | HF affects neither the $Na^+–Ca^{2+}$ exchange current (I_{NCX}) nor its $[Ca^{2+}]_i$ dependency. (A) Voltage clamp protocol used. **(B)** Typical changes in $[Ca^{2+}]_i$ and I_{NCX} (gray and black traces, respectively) in response to the voltage clamp protocol of **(A)**. **(C)** Average I_{NCX}-$[Ca^{2+}]_i$ relationships obtained during the repolarization-induced $[Ca^{2+}]_i$ decline. Solid lines: linear fits. **(D)** Average time constants of the $[Ca^{2+}]_i$ and I_{NCX} decline during the repolarizing step to −60 mV.

now also the late diastolic $[Ca^{2+}]_i$ rise is significantly lower in HF SAN cells (**Figure 5B**, bottom right).

Muscarinic receptor stimulation with 50 nM acetylcholine significantly decreased the frequency and $[Ca^{2+}]_i$ transients parameters in both CTRL and HF SAN cells, with exception of the time constant of decay which was significantly increased in both groups of cells (**Figure 6**). In presence of acetylcholine, only the frequency differs significantly between HF and CTRL SAN cells.

From these data we conclude that HF does not affect importantly the $[Ca^{2+}]_i$ modulation by acethylcholine and noradrenaline. However, in presence of noradrenaline, HF SAN cells have a reduced late diastolic $[Ca^{2+}]_i$ rise compared to CTRL SAN cells and this might have implications for pacemaker activity formation during β-adrenergic stimulation.

EFFECTS OF HF ON THE I_{NCX} DURING THE DIASTOLIC DEPOLARIZATION PHASE

The $[Ca^{2+}]_i$ transients are longer in HF SAN cells, likely due to reduced SERCA activity. In general, it is assumed that this will promote NCX mediated Ca^{2+} extrusion, and thus will increase the I_{NCX}-mediated net inward current during the diastolic depolarization (Ju and Allen, 1998; Sanders et al., 2006; Lau et al., 2011). Such an effect may, at least partially, counteract the previously observed decrease in I_f-mediated inward current in our used model of HF (Verkerk et al., 2003). However, NCX function during the cardiac cycle is not only determined by $[Ca^{2+}]_i$,

but also by the intracellular Na^+ ($[Na^+]_i$) concentration, and the membrane potential (V_m) (Blaustein and Lederer, 1999).

Next, we recorded action potentials (APs) simultaneously with $[Ca^{2+}]_i$ in combined $[Ca^{2+}]_i$ and patch clamp experiments, and calculated I_{NCX} during SAN APs using the measured $[Ca^{2+}]_i$ and V_m. Combined $[Ca^{2+}]_i$ and patch clamp experiments were performed in 7 CTRL and 5 HF SAN cells. The average $[Ca^{2+}]_i$ transient and AP parameters recapitulate the CTRL and HF SAN cell phenotype of the present paper (**Figure 1**) and of our previous study (Verkerk et al., 2003; **Figure 1**), although the differences in frequency and diastolic depolarization rate between CTRL and HF SAN cells did not reach the level of statistical significance due to the small number of cells (data not shown). **Figures 7A,B**, show a selected AP and $[Ca^{2+}]_i$ transient of a CTRL and HF SAN cell, which closely represent the mean differences in $[Ca^{2+}]_i$ transient and AP properties. **Figure 7C** shows the reconstructed I_{NCX}, based on the simultaneously recorded Ca^{2+} transients and APs of **Figures 7A,B**. In the CTRL SAN cell, I_{NCX} is inward for the entire AP, with a small amplitude early in the AP and a maximal amplitude late during repolarization. The I_{NCX} declined during the diastolic depolarization phase, consistent with the decrease in $[Ca^{2+}]_i$. In HF, I_{NCX} during the AP is close to that of the CTRL SAN cells, except that the amplitude is slightly larger during the diastolic depolarization. This is likely due to the slightly higher $[Ca^{2+}]_i$ in the diastolic depolarization phase, since the APs were almost identical and an identical $[Na^+]_i$ concentration of 5 mM was used for CTRL and HF SAN cells in both the pipette solution and calculations. **Figure 7D** extends our analysis to an increased $[Na^+]_i$, as frequently observed in ventricular myocytes of our used HF model (Baartscheer et al., 2003b). Elevation of the $[Na^+]_i$ by 50% to 7.5 mM, in line with the observations of Baartscheer et al. (2003b), decreased the diastolic I_{NCX} in both CTRL and HF SAN cells. Interestingly, I_{NCX} may become even shortly outward early during the AP. **Figure 7E** shows the I_{NCX} of the CTRL SAN cell with 5 mM $[Na^+]_i$ and the I_{NCX} of the HF SAN cell with 7.5 mM $[Na^+]_i$. It is evident that under these conditions I_{NCX} in HF SAN cell is close to that of the CTRL SAN, except for the outward I_{NCX} in the HF SAN cell. Similar results are obtained with the NCX model equations of Faber and Rudy (2000) (data not shown).

From these data we conclude that the decreased $[Ca^{2+}]_i$ transient decay in HF may result in slightly increased I_{NCX} during the diastolic depolarization phase, but that this effect is counteracted by a HF-induced increase in $[Na^+]_i$.

DISCUSSION

In the present study, we characterized the $[Ca^{2+}]_i$ cycling of single SAN cells isolated from CTRL rabbits and rabbits with volume and pressure overload-induced HF. The mechanisms behind $[Ca^{2+}]_i$ cycling in ventricular myocytes are diverse and complex (for reviews, see Guatimosim et al., 2002; Eisner et al., 2005; Bers, 2006b; Neef and Maier, 2013). In short, the $[Ca^{2+}]_i$ transient is triggered by Ca^{2+} influx through sarcolemmal Ca^{2+} channels, which results in release of Ca^{2+} from the SR via ryanodine-2 (RyR2) channels. This so-called Ca^{2+}-induced Ca^{2+} release (CICR) is importantly modulated by T-tubuli organization, with co-localization of $I_{Ca,L}$ and RyR2 channels (Øyehaug et al., 2013),

FIGURE 5 | Effects of 500 nM noradrenaline (NA) on the [Ca^{2+}]$_i$ transient parameters in CTRL and HF SAN cells. (A) Representative [Ca^{2+}]$_i$ transients in absence (solid lines) and presence (dashed lines) of NA. **(B)** Average [Ca^{2+}]$_i$ transient characteristics in absence and presence of NA. *$P < 0.05$.
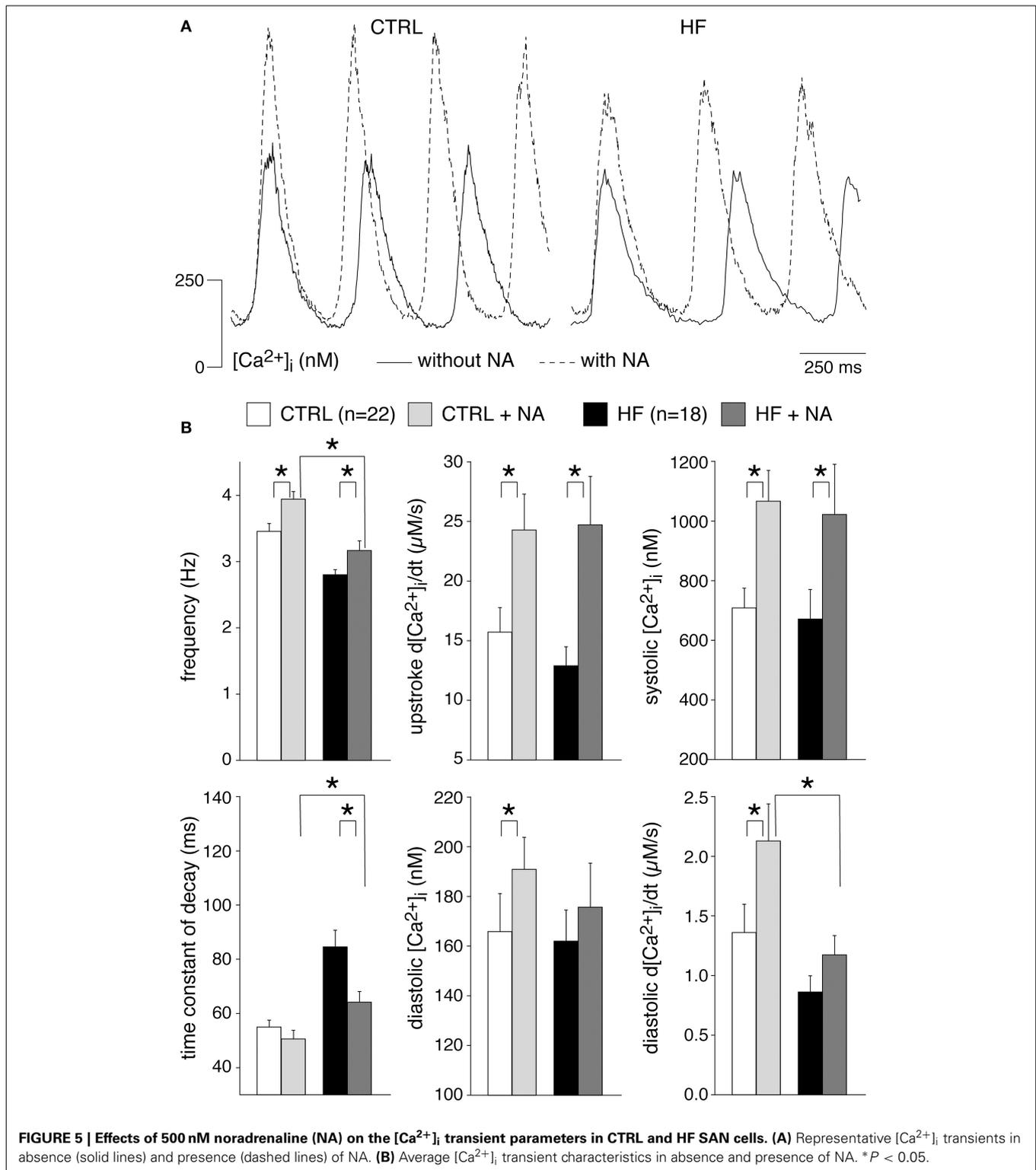
and the open probability of RyR2 channels (Guatimosim et al., 2002). The amplitude of the [Ca^{2+}]$_i$ transient depends importantly on the SR Ca^{2+} content (Bassani et al., 1992; Trafford et al., 2000, 2001; Díaz et al., 2004; Dibb et al., 2007; Briston et al., 2011). The decline of the [Ca^{2+}]$_i$ transient is mainly due

to SR Ca^{2+} reuptake through SERCA and extrusion of Ca^{2+} via the NCX. Because NCX and SERCA activity compete during the decline of the [Ca^{2+}]$_i$ transient, any change in SERCA function indirectly affects NCX contribution and vice versa, resulting in changes in the Ca^{2+} content of the SR and consequently

FIGURE 6 | Effects of 50 nM acetylcholine (ACh) on the $[Ca^{2+}]_i$ transient parameters in CTRL and HF SAN cells. (A) Representative $[Ca^{2+}]_i$ transients in absence (solid lines) and presence (dashed lines) of ACh. **(B)** Average $[Ca^{2+}]_i$ transient characteristics in absence and presence of ACh. $*P < 0.05$.
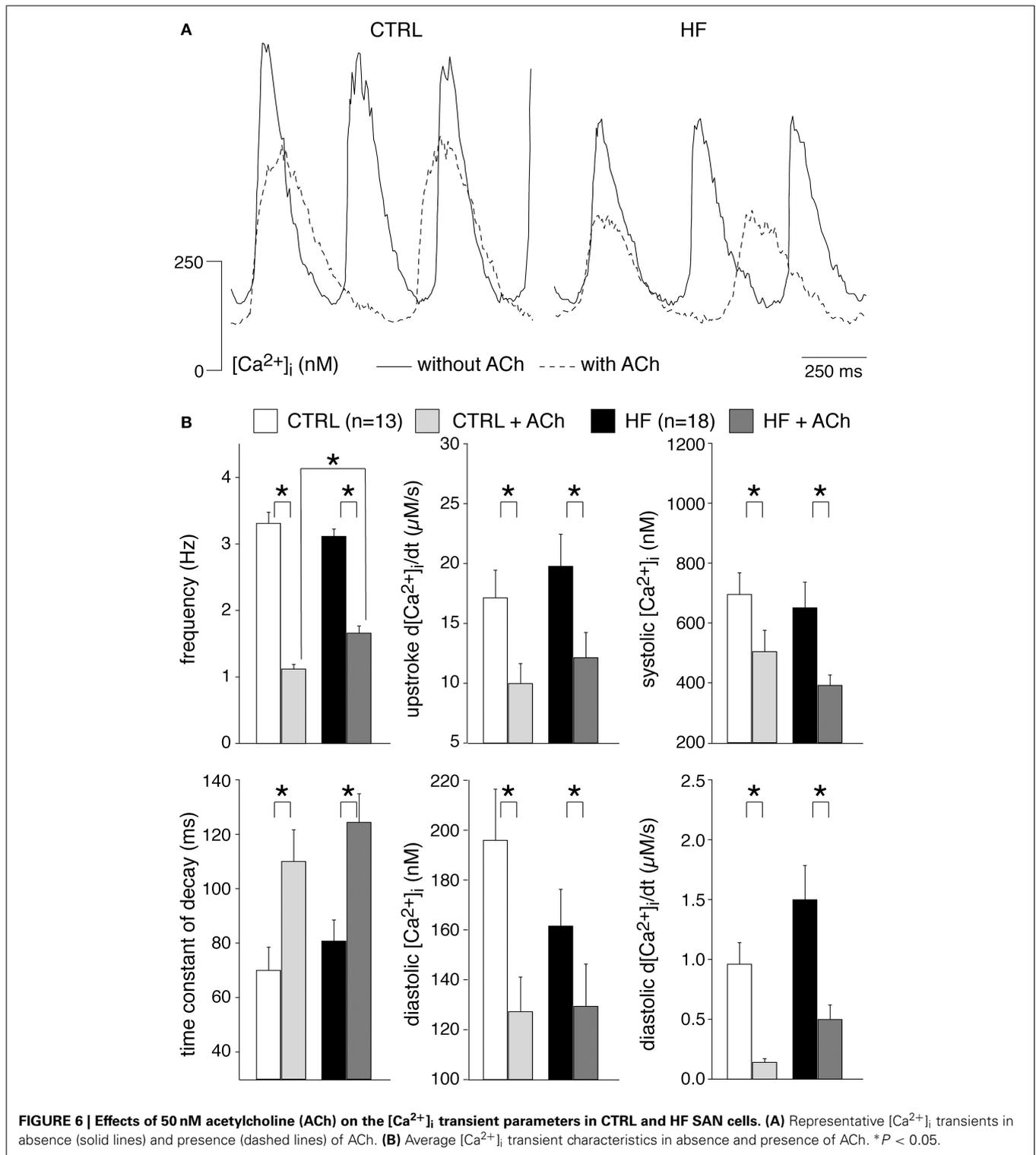
$[Ca^{2+}]_i$ transient amplitudes (Eisner et al., 2005; Bers, 2006a; Neef and Maier, 2013). The diastolic Ca^{2+} concentration is regulated by the $[Ca^{2+}]_i$ transient decline, especially during rapid pacing (Laurita et al., 2003), and leak of RyR2 channels (Neef and Maier, 2013). Both a slower $[Ca^{2+}]_i$ transient decay and increased RyR2 channel leak results in elevation of the diastolic Ca^{2+} concentration. SAN cells exhibit also another $[Ca^{2+}]_i$ transient characteristic, i.e., rise of the diastolic $[Ca^{2+}]_i$, which is a key signature of pacemaking by the Ca^{2+} clock (for review, see Maltsev and Lakatta, 2008; Lakatta et al., 2010; Joung et al., 2011).
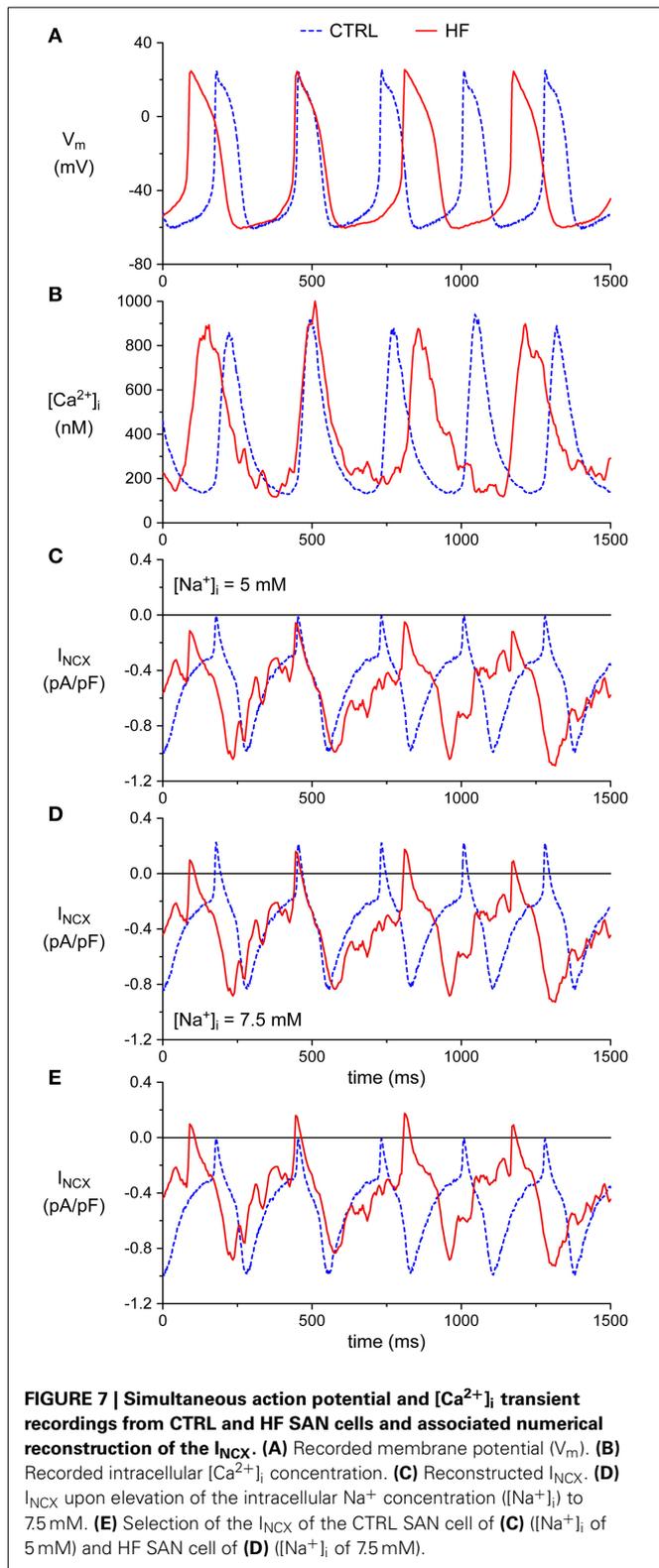
FIGURE 7 | Simultaneous action potential and [Ca²⁺]i transient recordings from CTRL and HF SAN cells and associated numerical reconstruction of the INCX. **(A)** Recorded membrane potential (Vm). **(B)** Recorded intracellular [Ca²⁺]i concentration. **(C)** Reconstructed INCX. **(D)** INCX upon elevation of the intracellular Na⁺ concentration ([Na⁺]i) to 7.5 mM. **(E)** Selection of the INCX of the CTRL SAN cell of **(C)** ([Na⁺]i of 5 mM) and HF SAN cell of **(D)** ([Na⁺]i of 7.5 mM).

(Guatimosim et al., 2002). An increase of RyR2 open probability, as may occur during HF in ventricular myocytes, also leads to an increased amount of Ca²⁺ sparks, resulting in an increased diastolic [Ca²⁺]i concentration and reduced SR Ca²⁺ content since more Ca²⁺ is pumped out of the cell by the NCX (Neef and Maier, 2013). Furthermore, HF in ventricular mycoytes typically slows the [Ca²⁺]i transient decay due to reduced SERCA function. Such reduced Ca²⁺ uptake by SERCA, in combination with a frequently observed upregulation of the NCX and consequently increased Ca²⁺ efflux, will reduce the SR Ca²⁺ content and systolic Ca²⁺ transient amplitude (for reviews, see Bers, 2006b; Eisner et al., 2013; Neef and Maier, 2013). Of note, the diastolic [Ca²⁺]i concentration is frequently elevated by HF, due to the slower [Ca²⁺]i transient decay and increased RyR2 channel leak.

We found that HF SAN cells have (1) a reduced frequency of spontaneous [Ca²⁺]i transients, (2) a slower [Ca²⁺]i transient decay, and (3) a reduced diastolic [Ca²⁺]i rise during β-adrenergic stimulation, compared to CTRL SAN cells. Combined action potential and [Ca²⁺]i measurements demonstrated that the decreased [Ca²⁺]i transient decay in HF SAN cells may result in slightly increased INCX during the diastolic depolarization phase, but that this effect is counteracted by HF-induced increase in [Na⁺]i.

INTRINSIC CYCLE LENGTH IS PROLONGED IN HF SAN CELLS
We found a lower frequency of spontaneous [Ca²⁺]i transients in HF SAN cells, indicating that intrinsic cycle length was prolonged in HF SAN cells (**Figure 1**). This finding agrees with previously findings in intact SAN (Opthof et al., 2000) and single SAN cells (Verkerk et al., 2003) of rabbit. The frequency of the intrinsic cycle length based on the [Ca²⁺]i transients was 14% slower in HF SAN cells (**Figure 1**) and this percentage closely matches the increased intrinsic cycle length (15%) of our previous study with the same rabbit HF model and measured with perforated patch clamp methodology (Verkerk et al., 2003).

We found that the frequency of the spontaneous [Ca²⁺]i transients in both CTRL and HF SAN cells influenced various [Ca²⁺]i transient characteristics, including diastolic and systolic [Ca²⁺]i concentrations, systolic [Ca²⁺]i rise and decay, and late diastolic [Ca²⁺]i rise (**Figure 2**, **Table 2**). All parameters, except the [Ca²⁺]i transient time constant of decay, increased upon increased frequencies. The frequency dependency was not significantly different in HF compared to CTRL SAN cells (**Figure 2**, **Table 2**). Nevertheless, the frequency dependency relationships might have influenced some principal findings because spontaneous activity is lower in HF SAN cells. The relative small difference in intrinsic cycle length of CTRL and HF SAN cells, the rather large variation between cells, and the modest steepness of the frequency-dependencies (**Table 2**, **Figure 2**) may all have contributed to the absence of significant differences in frequency dependency between HF and CTRL SAN cells.

Recently, Herrmann et al. elegantly solved the problem of intrinsic rate differences in SAN cells by using electrical field stimulation (Herrmann et al., 2013). Using this approach, they investigated the contribution of the murine sodium-calcium exchanger

HF in ventricular myocytes may affect many [Ca²⁺]i transient characteristics. It is reported that HF decreases the upstroke velocity of the [Ca²⁺]i transient by T-tubuli disorganization (Øyehaug et al., 2013) and increased open probability of RyR2 channels

protein NCX1 to cardiac pacemaking in transgenic mice selectively lacking NCX1 in the cardiac pacemaking and conduction system. Among other things, they found that $[Ca^{2+}]_i$ transients measured during electrical field stimulation were of smaller magnitude and decelerated kinetics in NCX1 knockout cells.

$[Ca^{2+}]_i$ TRANSIENT CHARACTERISTICS IN HF SAN CELLS
$[Ca^{2+}]_i$ transient under basal conditions
We observed that HF results in a slower $[Ca^{2+}]_i$ transient decay (**Figure 1**). The $[Ca^{2+}]_i$ transient time constant of decay was increased by 41% in HF cells, which is larger than expected from the $[Ca^{2+}]_i$ transient time constant of decay vs. frequency relationship that explains only a $\approx 17\%$ difference. HF affected neither the I_{NCX} density and I_{NCX}-$[Ca^{2+}]_i$ relationship (**Figure 4**) nor the mitochondrial Ca^{2+} uptake and sarcolemmal Ca-ATPase (**Figure 3**), indicating that downregulation of SERCA activity also contributes to the slower $[Ca^{2+}]_i$ transient decay. Any contribution of (changes in) T-tubular organization, sarcolemmal calcium currents, and action potential duration can be ruled out because T-tubuli are absent in rabbit SAN cells (Masson-Pévet et al., 1979), and $I_{Ca,T}$ and $I_{Ca,L}$ densities as well as action potential duration are unaffected in HF rabbit SAN cells (Verkerk et al., 2003).

HF in SAN cells did not affect the diastolic and systolic $[Ca^{2+}]_i$ concentrations, systolic $[Ca^{2+}]_i$ rise, late diastolic $[Ca^{2+}]_i$ rise (**Figure 1**), and SR Ca^{2+} content (**Figure 3**). The unaffected diastolic Ca^{2+} concentration, at first sight, might appear to be inconsistent with the decrease of the $[Ca^{2+}]_i$ transient decline. It should be noted, however, that HF SAN cells have a lower frequency due to their longer diastolic depolarization phase (Verkerk et al., 2003), which leaves more time for Ca^{2+} reuptake and/or removal. The unchanged slope of the LDCAE, associated with LCRs and Ca^{2+} sparks, suggests that RyR2 open probability is not affected in HF SAN cells. Our finding contrasts findings in a canine model of rapid pacing-induced heart failure, where it was found, using isolated right atrial preparations, that LDCAE was reduced (Shinohara et al., 2010). Differences in HF model, species and preparations might contribute to the contrasting findings.

The unaltered SR Ca^{2+} content agrees with the unaffected $[Ca^{2+}]_i$ transient amplitude in HF SAN cells, but is somewhat surprising given that reduced SERCA activity is supposed to result in a lower SR Ca^{2+} content. The latter is due because NCX and SERCA activity compete for Ca^{2+} during the $[Ca^{2+}]_i$ transient decline, and reduced SERCA function thus indirectly favors greater Ca^{2+} efflux via the NCX (for reviews, see Guatimosim et al., 2002; Eisner et al., 2005; Bers, 2006b; Neef and Maier, 2013). We observed a similar SR Ca^{2+} content in HF and CTRL SAN cells despite the slower $[Ca^{2+}]_i$ transient decline in HF SAN cells. This suggests a compensatory increase in Ca^{2+} influx. $I_{Ca,T}$ and $I_{Ca,L}$ densities were not affected in HF SA node cells (Verkerk et al., 2003), but we cannot exclude that the longer diastolic depolarization phase in HF SAN cells (Verkerk et al., 2003) may result in a larger background Ca^{2+} influx via L-type Ca^{2+} channels (Verheijck et al., 1999). Alternatively, increased $[Na^+]_i$ as occurs during HF may promote Ca^{2+} influx via reversed NCX activity (Despa et al., 2002). Indeed, by reconstruction of the I_{NCX}, based on action potentials and simultaneously measured $[Ca^{2+}]_i$

transients, we found that the I_{NCX} became outward, thus resulting in Ca^{2+} influx, early during the AP (**Figures 7D,E**) under conditions of elevated $[Na^+]_i$ as occur during HF.

$[Ca^{2+}]_i$ transient during β-adrenergic and muscarinic receptor stimulation
We found that the β-adrenergic and muscarinic receptor stimulation was hardly affected by HF. In both CTRL and HF SAN cells, acetylcholine significantly decreased the frequency and $[Ca^{2+}]_i$ transients parameters, with exception of the time constant of decay which was significantly increased in both groups of cells (**Figure 6**). The ACh induced effects were largely similar in CTRL and HF SAN cells. Noradrenaline, on the other hand, significantly increased the frequency and most $[Ca^{2+}]_i$ transient parameters in both CTRL and HF SAN cells (**Figure 5**), leading to preserved $[Ca^{2+}]_i$ transient differences between the CTRL and the HF SAN cells. However, in presence of noradrenaline the late diastolic $[Ca^{2+}]_i$ rise was significantly lower in HF SAN cells compared to HF SAN cells. The lower late diastolic $[Ca^{2+}]_i$ rise in HF SAN cells in presence of noradrenaline is in agreement with findings in canine right atrial preparations by Shinohara et al. (2010).

IMPLICATION OF HF-INDUCED $[Ca^{2+}]_i$ TRANSIENT CHANGES IN PACEMAKER ACTIVITY
Overall, the effects of HF on $[Ca^{2+}]_i$ transients in rabbit SAN cells were modest. The decrease in frequency of the spontaneous $[Ca^{2+}]_i$ transient in HF SAN cells is completely explained by the previously observed slower intrinsic cycle length (Verkerk et al., 2003). The slower $[Ca^{2+}]_i$ transient decay will promote Ca^{2+} transport across the sarcolemma by the NCX (Bers et al., 2006), an electrogenic process that delivers inward current at diastolic potentials. The observed slower $[Ca^{2+}]_i$ transient decay may thus result in increased I_{NCX} during the diastolic depolarization phase, thereby partially counteracting the previously observed decrease in I_f-mediated inward current in HF (Verkerk et al., 2003). Indeed, reconstructed I_{NCX}, based on the simultaneously recorded Ca^{2+} transients and APs, demonstrated a slightly larger amplitude during the diastolic depolarization phase (**Figure 7C**). However, when we incorporated an increased $[Na^+]_i$, as frequently observed in ventricular myocytes, including those from our rabbit HF model (Baartscheer et al., 2003b), the I_{NCX} in the diastolic depolarization phase is close to that of the CTRL SAN (**Figure 7E**). Thus, the slower $[Ca^{2+}]_i$ transient decay in HF has likely a limited role in the slower intrinsic cycle length in HF SAN cells. The slope of late diastolic $[Ca^{2+}]_i$ elevation, associated with localized Ca^{2+} releases (LCRs) or Ca^{2+} sparks (Bogdanov et al., 2006; Maltsev et al., 2006; Joung et al., 2009, 2010; van Borren et al., 2010), was unaffected under basal conditions, suggesting that the Ca^{2+} clock is not the primary cause of the slower intrinsic cycle length in HF SAN cells. Considering the importance of late diastolic $[Ca^{2+}]_i$ rise in setting pacemaker activity, however, the lower late diastolic $[Ca^{2+}]_i$ rise in HF SAN cells in presence of noradrenaline suggest that an impaired increase in intrinsic frequency under such conditions may be related to reduced Ca^{2+} clock function.

LIMITATIONS

We used indo-1 to measure [Ca^{2+}]$_i$, because this ratiometric indicator is less prone to cell contractions and loss of dye. However, indo-1 had an adverse effect on cell viability and rendered many smaller cells quiescent (Lancaster et al., 2004). We cannot rule out the possibility that indo-1 has affected the principal findings, but we assume that its effect is limited because the differences in spontaneous activity of CTRL and HF SAN cells in our present study are highly similar to the differences that we observed with perforated patch clamp measurements (Verkerk et al., 2003).

In our study, we used the complete SAN for cell isolation. However, the SAN is not homogeneous in its composition. This seems valid for membrane currents (Boyett et al., 2000), but also the expression of several calcium handling proteins varies across the node (Musa et al., 2002; Lancaster et al., 2004), all of which are expressed at a lower level in the center of the SAN compared with the periphery, although such findings are debated (Lyashkov et al., 2007). Cells from the center and periphery may differ in cell capacitance. We exclude cell location-dependency as an explanation for our principal findings because cell capacitance did not differ between control and HF.

We reconstructed I$_{NCX}$ based on simultaneous measurements of [Ca^{2+}]$_i$ and spontaneous action potentials as well as the [Na$^+$]$_i$ of 5 and 7.5 mM used in our pipette solution and found in our model of HF previously (Baartscheer et al., 2003b). Data on [Na$^+$]$_i$ in SAN cells are extremely sparse and we were not succesful in [Na$^+$]$_i$ measurements with benzofuran isophthalate (SBFI) ourselves. However, the used 5 mM [Na$^+$]$_i$ is close to the concentrations of 4.5 and 4.0 mM in rabbit multicellular SAN preparations and single SAN cells, respectively, found by Choi et al. (1999). In our reconstructions, we used the Lindblad et al. (1996) equations for I$_{NCX}$. We could not make use of I$_{NCX}$ equations from more recent models, in particular the rabbit SAN cell models by Maltsev and Lakatta (2010b) and Severi et al. (2012), because these require data on the concentration of Ca^{2+} in a sarcolemmal subspace rather than global [Ca^{2+}]$_i$.

CONCLUSIONS

In our rabbit model of HF, SAN cells have reduced SERCA activity and reduced intrinsic frequency, both resulting in a slower Ca^{2+} decay. The decreased [Ca^{2+}]$_i$ transient decay in HF SAN cells may result in slightly increased I$_{NCX}$ during the diastolic depolarization phase, but this effect is likely counteracted by HF-induced increase in [Na$^+$]$_i$. Reduced late diastolic [Ca^{2+}]$_i$ rise during β-adrenergic stimulation may contribute to the impaired increase in frequency under this condition in HF SAN cells.

REFERENCES

Allah, E. A., Tellez, J. O., Yanni, J., Nelson, T., Monfredi, O., Boyett, M. R., et al. (2011). Changes in the expression of ion channels, connexins and Ca^{2+}-handling proteins in the sino-atrial node during postnatal development. *Exp. Physiol.* 96, 426–438. doi: 10.1113/expphysiol.2010.055780

Arai, A., Kodama, I., and Toyama, J. (1996). Roles of Cl$^-$ channels and Ca^{2+} mobilization in stretch-induced increase of SA node pacemaker activity. *Am. J. Physiol.* 270, H1726–H1735.

Baartscheer, A., Schumacher, C. A., Belterman, C. N. W., Coronel, R., and Fiolet, J. W. T. (2003a). SR calcium handling and calcium after-transients in a rabbit model of heart failure. *Cardiovasc. Res.* 58, 99–108. doi: 10.1016/S0008-6363(02)00854-4

Baartscheer, A., Schumacher, C. A., van Borren, M. M. G. J., Belterman, C. N. W., Coronel, R., and Fiolet, J. W. T. (2003b). Increased Na$^+$/H$^+$-exchange activity is the cause of increased [Na$^+$]$_i$ and underlies disturbed calcium handling in the rabbit pressure and volume overload heart failure model. *Cardiovasc. Res.* 57, 1015–1024. doi: 10.1016/S0008-6363(02)00809-X

Bassani, R. A., Bassani, J. W. M., and Bers, D. M. (1992). Mitochondrial and sarcolemmal Ca^{2+} transport reduce [Ca^{2+}]$_i$ during caffeine contractures in rabbit cardiac myocytes. *J. Physiol.* 453, 591–608. doi: 10.1113/jphysiol.1992.sp019246

Bers, D. M., Despa, S., and Bossuyt, J. (2006). Regulation of Ca^{2+} and Na$^+$ in normal and failing cardiac myocytes. *Ann. N.Y. Acad. Sci.* 1080, 165–177. doi: 10.1196/annals.1380.015

Bers, D. M. (1987). Ryanodine and the calcium content of cardiac SR assessed by caffeine and rapid cooling contractures. *Am. J. Physiol.* 253, C408–C415.

Bers, D. M. (2006a). The beat goes on: diastolic noise that just won't quit. *Circ. Res.* 99, 921–923. doi: 10.1161/01.RES.0000249859.10103.a9

Bers, D. M. (2006b). Altered cardiac myocyte Ca regulation in heart failure. *Physiology (Bethesda)* 21, 380–387. doi: 10.1152/physiol.00019.2006

Blaustein, M. P., and Lederer, W. J. (1999). Sodium/calcium exchange: its physiological implications. *Physiol. Rev.* 79, 763–854.

Bogdanov, K. Y., Maltsev, V. A., Vinogradova, T. M., Lyashkov, A. E., Spurgeon, H. A., Stern, M. D., et al. (2006). Membrane potential fluctuations resulting from submembrane Ca^{2+} releases in rabbit sinoatrial nodal cells impart an exponential phase to the late diastolic depolarization that controls their chronotropic state. *Circ. Res.* 99, 979–987. doi: 10.1161/01.RES.0000247933.66532.0b

Boyett, M. R., Honjo, M., and Kodama, I. (2000). The sinoatrial node, a heterogeneous pacemaker structure. *Cardiovasc. Res.* 47, 658–687. doi: 10.1016/S0008-6363(00)00135-8

Briston, S. J., Caldwell, J. L., Horn, M. A., Clarke, J. D., Richards, M. A., Greensmith, D. J., et al. (2011). Impaired β-adrenergic responsiveness accentuates dysfunctional excitation–contraction coupling in an ovine model of tachypacing-induced heart failure. *J. Physiol.* 589, 1367–1382. doi: 10.1113/jphysiol.2010.203984

Choi, S., Wang, D. Y., Noble, D., and Lee, C. O. (1999). Effect of isoprenaline, carbachol, and Cs$^+$ on Na$^+$ activity and pacemaker potential in rabbit SA node cells. *Am. J. Physiol.* 276, H205–H214.

Despa, S., Islam, M. A., Weber, C. R., Pogwizd, S. M., and Bers, D. M. (2002). Intracellular Na$^+$ concentration is elevated in heart failure but Na/K pump function is unchanged. *Circulation* 105, 2543–2548. doi: 10.1161/01.CIR.0000016701.85760.97

Díaz, M. E., Graham, H. K., and Trafford, A. W. (2004). Enhanced sarcolemmal Ca^{2+} efflux reduces sarcoplasmic reticulum Ca^{2+} content and systolic Ca^{2+} in cardiac hypertrophy. *Cardiovasc. Res.* 62, 538–547. doi: 10.1016/j.cardiores.2004.01.038

Dibb, K. M., Eisner, D. A., and Trafford, A. W. (2007). Regulation of systolic [Ca^{2+}]$_i$ and cellular Ca^{2+} flux balance in rat ventricular myocytes by SR Ca^{2+}, L-type Ca^{2+} current and diastolic [Ca^{2+}]$_i$. *J. Physiol.* 585, 579–592. doi: 10.1113/jphysiol.2007.141473

DiFrancesco, D. (2010). Considerations on the size of currents required for pacemaking. *J. Mol. Cell. Cardiol.* 48, 802–803. doi: 10.1016/j.yjmcc.2009.11.022

DiFrancesco, D., and Noble, D. (2012a). The funny current has a major pacemaking role in the sinus node. *Heart Rhythm* 9, 299–301. doi: 10.1016/j.hrthm.2011.09.021

DiFrancesco, D., and Noble, D. (2012b). Rebuttal: "The funny current in the context of the coupled clock pacemaker cell system." *Heart Rhythm* 9, 457–458. doi: 10.1016/j.hrthm.2011.09.023

DiFrancesco, D., and Robinson, R. B. (2002). β-Modulation of pacemaker rate: novel mechanism or novel mechanics of an old one? *Circ. Res.* 90:e69. doi: 10.1161/01.RES.0000014803.05780.E7

Du, Y., Huang, X., Wang, T., Han, K., Zhang, J., Xi, Y., et al. (2007). Downregulation of neuronal sodium channel subunits Na$_v$1.1 and Na$_v$1.6 in the sinoatrial node from volume-overloaded heart failure rat. *Pflügers Arch.* 454, 451–459. doi: 10.1007/s00424-007-0216-4

Eisner, D., Caldwell, J., and Trafford, A. (2013). Sarcoplasmic reticulum Ca-ATPase and heart failure 20 years later. *Circ. Res.* 113, 958–961. doi: 10.1161/CIRCRESAHA.113.302187

Eisner, D. A., Diaz, M. E., Li, Y., O'Neill, S. C., and Trafford, A. W. (2005). Stability and instability of regulation of intracellular calcium. *Exp. Physiol.* 90, 3–12. doi: 10.1113/expphysiol.2004.029231

Faber, G. M., and Rudy, Y. (2000). Action potential and contractility changes in $[Na^+]_i$ overloaded cardiac myocytes: a simulation study. *Biophys. J.* 78, 2392–2404. doi: 10.1016/S0006-3495(00)76783-X

Guatimosim, S., Dilly, K., Santana, L. F., Jafri, M. S., Sobie, E. A., and Lederer, W. J. (2002). Local Ca^{2+} signaling and EC coupling in heart: Ca^{2+} sparks and the regulation of the $[Ca^{2+}]_i$ transient. *J. Mol. Cell. Cardiol.* 34, 941–950. doi: 10.1006/jmcc.2002.2032

Herrmann, S., Lipp, P., Wiesen, K., Stieber, J., Nguyen, H., Kaiser, E., et al. (2013). The cardiac sodium-calcium exchanger NCX1 is a key player in the initiation and maintenance of a stable heart rhythm. *Cardiovasc. Res.* 99, 780–788. doi: 10.1093/cvr/cvt154

Himeno, Y., Toyoda, F., Matsuura, H., and Noma, A. (2011a). Reply to "Letter to the editor: 'Validating the requirement for beat-to-beat coupling of the Ca^{2+} clock and M clock in pacemaker cell normal automaticity.'" *Am. J. Physiol. Heart Circ. Physiol.* 300, H2325–H2326. doi: 10.1152/ajpheart.00317.2011

Himeno, Y., Toyoda, F., Satoh, H., Amano, A., Cha, C. Y., Matsuura, H., et al. (2011b). Minor contribution of cytosolic Ca^{2+} transients to the pacemaker rhythm in guinea pig sinoatrial node cells. *Am. J. Physiol. Heart Circ. Physiol.* 300, H251–H261. doi: 10.1152/ajpheart.00764.2010

Honjo, H., Inada, S., Lancaster, M. K., Yamamoto, M., Niwa, R., Jones, S. A., et al. (2003). Sarcoplasmic reticulum Ca^{2+} release is not a dominating factor in sinoatrial node pacemaker activity. *Circ. Res.* 92, e41–e44. doi: 10.1161/01.RES.0000055904.21974.BE

Hove-Madsen, L., and Tort, L. (2001). Characterization of the relationship between Na^+-Ca^{2+} exchange rate and cytosolic calcium in trout cardiac myocytes. *Pflügers Arch.* 441, 701–708. doi: 10.1007/s004240000470

Hussain, M., Drago, G. A., Colyer, J., and Orchard, C. H. (1997). Rate-dependent abbreviation of Ca^{2+} transient in rat heart is independent of phospholamban phosphorylation. *Am. J. Physiol.* 273, H695–H706.

Joung, B., Chen, P.-S., and Lin, S.-F. (2011). The role of the calcium and the voltage clocks in sinoatrial node dysfunction. *Yonsei Med. J.* 52, 211–219. doi: 10.3349/ymj.2011.52.2.211

Joung, B., Lin, S.-F., Chen, Z., Antoun, P. S., Maruyama, M., Han, S., et al. (2010). Mechanisms of sinoatrial node dysfunction in a canine model of pacing-induced atrial fibrillation. *Heart Rhythm* 7, 88–95. doi: 10.1016/j.hrthm.2009.09.018

Joung, B., Tang, L., Maruyama, M., Han, S., Chen, Z., Stucky, M., et al. (2009). Intracellular calcium dynamics and acceleration of sinus rhythm by β-adrenergic stimulation. *Circulation* 119, 788–796. doi: 10.1161/CIRCULATIONAHA.108.817379

Ju, Y.-K., and Allen, D. G. (1998). Intracellular calcium and Na^+-Ca^{2+} exchange current in isolated toad pacemaker cells. *J. Physiol.* 508, 153–166. doi: 10.1111/j.1469-7793.1998.153br.x

Kho, C., Lee, A., and Hajjar, R. J. (2012). Altered sarcoplasmic reticulum calcium cycling – targets for heart failure therapy. *Nat. Rev. Cardiol.* 9, 717–733. doi: 10.1038/nrcardio.2012.145

Kodama, I., Honjo, H., and Boyett, M. R. (2002). Are we lost in the labyrinth of the sinoatrial node pacemaker mechanism? *J. Cardiovasc. Electrophysiol.* 13, 1303–1305. doi: 10.1046/j.1540-8167.2002.01303.x

Lacinová, L., Kurejová, M., Klugbauer, N., and Hofmann, F. (2006). Gating of the expressed T-type $Ca_v3.1$ calcium channels is modulated by Ca^{2+}. *Acta. Physiol.* 186, 249–260. doi: 10.1111/j.1748-1716.2006.01539.x

Lakatta, E. G., and DiFrancesco, D. (2009). What keeps us ticking: a funny current, a calcium clock, or both? *J. Mol. Cell. Cardiol.* 47, 157–170. doi: 10.1016/j.yjmcc.2009.03.022

Lakatta, E. G., and Maltsev, V. A. (2012). Rebuttal: what I$_f$ the shoe doesn't fit? "The funny current has a major pacemaking role in the sinus node." *Heart Rhythm* 9, 459–460. doi: 10.1016/j.hrthm.2011.09.024

Lakatta, E. G., Maltsev, V. A., Bogdanov, K. Y., Stern, M. D., and Vinogradova, T. (2003). Cyclic variation of intracellular calcium: a critical factor for cardiac pacemaker cell dominance. *Circ. Res.* 92, e45–e50. doi: 10.1161/01.RES.0000055920.64384.FB

Lakatta, E. G., Maltsev, V. A., and Vinogradov, T. M. (2010). A coupled SYSTEM of intracellular Ca^{2+} clocks and surface membrane voltage clocks controls the timekeeping mechanism of the heart's pacemaker. *Circ. Res.* 106, 659–673. doi: 10.1161/CIRCRESAHA.109.206078

Lancaster, M. K., Jones, S. A., Harrison, S. M., and Boyett, M. R. (2004). Intracellular Ca^{2+} and pacemaking within the rabbit sinoatrial node: heterogeneity of role and control. *J. Physiol.* 556, 481–494. doi: 10.1113/jphysiol.2003.057372

Lau, D. H., Roberts-Thomson, K. C., and Sanders, P. (2011). Sinus node revisited. *Curr. Opin. Cardiol.* 26, 55–59. doi: 10.1097/HCO.0b013e32834138f4

Laurita, K. R., Katra, R., Wible, B., Wan, X. P., and Koo, M. H. (2003). Transmural heterogeneity of calcium handling in canine. *Circ. Res.* 92, 668–675. doi: 10.1161/01.RES.0000062468.25308.27

Lei, M., Brown, H. F., and Terrar, D. A. (2000). Modulation of delayed rectifier potassium current, i_K, by isoprenaline in rabbit isolated pacemaker cells. *Exp. Physiol.* 85, 27–35. doi: 10.1111/j.1469-445X.2000.01915.x

Li, J., Qu, J., and Nathan, R., D (1997). Ionic basis of ryanodine's negative chronotropic effect on pacemaker cells isolated from the sinoatrial node. *Am. J. Physiol.* 273, H2481–H2489.

Lindblad, D. S., Murphey, C. R., Clark, J. W., and Giles, W. R. (1996). A model of the action potential and underlying membrane currents in a rabbit atrial cell. *Am. J. Physiol.* 271, H1666–H1696.

Lipsius, S. L., and Bers, D. M. (2003). Cardiac pacemaking: I$_f$ vs. Ca^{2+}, is it really that simple? *J. Mol. Cell. Cardiol.* 35, 891–893. doi: 10.1016/S0022-2828(03)00184-6

Luo, M., and Anderson, M. E. (2013). Mechanisms of altered Ca^{2+} handling in heart failure. *Circ. Res.* 113, 690–708. doi: 10.1161/CIRCRESAHA.113.301651

Lyashkov, A. E., Juhaszova, M., Dobrzynski, H., Vinogradova, T. M., Maltsev, V. A., Juhasz, O., et al. (2007). Calcium cycling protein density and functional importance to automaticity of isolated sinoatrial nodal cells are independent of cell size. *Circ. Res.* 100, 1723–1731. doi: 10.1161/CIRCRESAHA.107.153676

Maltsev, V. A., and Lakatta, E. G. (2008). Dynamic interactions of an intracellular Ca^{2+} clock and membrane ion channel clock underlie robust initiation and regulation of cardiac pacemaker function. *Cardiovasc. Res.* 77, 274–284. doi: 10.1093/cvr/cvm058

Maltsev, V. A., and Lakatta, E. G. (2010a). Funny current provides a relatively modest contribution to spontaneous beating rate regulation of human and rabbit sinoatrial node cells. *J. Mol. Cell. Cardiol.* 48, 804–806. doi: 10.1016/j.yjmcc.2009.12.009

Maltsev, V. A., and Lakatta, E. G. (2010b). A novel quantitative explanation for the autonomic modulation of cardiac pacemaker cell automaticity via a dynamic system of sarcolemmal and intracellular proteins. *Am. J. Physiol. Heart Circ. Physiol.* 298, H2010–H2023. doi: 10.1152/ajpheart.00783.2009

Maltsev, V. A., and Lakatta, E. G. (2012). The funny current in the context of the coupled-clock pacemaker cell system. *Heart Rhythm* 9, 302–307. doi: 10.1016/j.hrthm.2011.09.022

Maltsev, V. A., Vinogradova, T. M., and Lakatta, E. G. (2006). The emergence of a general theory of the initiation and strength of the heartbeat. *J. Pharmacol. Sci.* 100, 338–369. doi: 10.1254/jphs.CR0060018

Maltsev, V. A., Vinogradova, T. M., Stern, M. D., and Lakatta, E. G. (2011). Validating the requirement for beat-to-beat coupling of the Ca^{2+} clock and M clock in pacemaker cell normal automaticity. *Am. J. Physiol. Heart Circ. Physiol.* 300, H2323–H2324. doi: 10.1152/ajpheart.00110.2011

Mangoni, M. E., and Nargeot, J. (2008). Genesis and regulation of the heart automaticity. *Physiol. Rev.* 88, 919–982. doi: 10.1152/physrev.00018.2007

Masson-Pévet, M., Bleeker, W. K., and Gros, D. (1979). The plasma membrane of leading pacemaker cells in the rabbit sinus node. A qualitative and quantitative ultrastructural analysis. *Circ. Res.* 45, 621–629. doi: 10.1161/01.RES.45.5.621

Musa, H., Lei, M., Honjo, H., Jones, S. A., Dobrzynski, H., Lancaster, M. K., et al. (2002). Heterogeneous expression of Ca^{2+} handling proteins in rabbit sinoatrial node. *J. Histochem. Cytochem.* 50, 311–324. doi: 10.1177/002215540205000303

Neef, S., and Maier, L. S. (2013). Novel aspects of excitation-contraction coupling in heart failure. *Basic Res. Cardiol.* 108:360. doi: 10.1007/s00395-013-0360-2

Opthof, T., Coronel, R., Rademaker, H. M., Vermeulen, J. T., Wilms-Schopman, F. J., and Janse, M. J. (2000). Changes in sinus node function in a rabbit model of heart failure with ventricular arrhythmias and sudden death. *Circulation* 101, 2975–2980. doi: 10.1161/01.CIR.101.25.2975

Øyehaug, L., Loose, K. Ø., Jølle, G. F., Røe, Å. T., Sjaastad, I., Christensen, G., et al. (2013). Synchrony of cardiomyocyte Ca^{2+} release is controlled by T-tubule organization, SR Ca^{2+} content, and ryanodine receptor Ca^{2+} sensitivity. *Biophys. J.* 104, 1685–1697. doi: 10.1016/j.bpj.2013.03.022

Rigg, L., Heath, B. M., Cui, Y., and Terrar, D. A. (2000). Localisation and functional significance of ryanodine receptors during β-adrenoceptor stimulation in the

guinea-pig sino-atrial node. *Cardiovasc. Res.* 48, 254–264. doi: 10.1016/S0008-6363(00)00153-X

Rigg, L., Mattick, P. A. D., Heath, B. M., and Terrar, D. A. (2003). Modulation of the hyperpolarization-activated current (I_f) by calcium and calmodulin in the guinea-pig sino-atrial node. *Cardiovasc. Res.* 57, 497–504. doi: 10.1016/S0008-6363(02)00668-5

Sanders, L., Rakovic, S., Lowe, M., Mattick, P. A., and Terrar, D. A. (2006). Fundamental importance of Na$^+$-Ca^{2+} exchange for the pacemaking mechanism in guinea-pig sino-atrial node. *J. Physiol.* 571, 639–649. doi: 10.1113/jphysiol.2005.100305

Severi, S., Fantini, M., Charawi, L. A., and DiFrancesco, D. (2012). An updated computational model of rabbit sinoatrial action potential to investigate the mechanisms of heart rate modulation. *J. Physiol.* 590, 4483–4499. doi: 10.1113/jphysiol.2012.229435

Shinohara, T., Park, H.-W., Han, S., Shen, M. J., Maruyama, M., Kim, D., et al. (2010). Ca^{2+} clock malfunction in a canine model of pacing-induced heart failure. *Am. J. Physiol. Heart. Circ. Physiol.* 299, H1805–H1811. doi: 10.1152/ajpheart.00723.2010

Sipido, K. R., Callewaert, G., and Carmeliet, E. (1995). Inhibition and rapid recovery of Ca^{2+} current during Ca^{2+} release from sarcoplasmic reticulum in guinea pig ventricular myocytes. *Circ. Res.* 76, 102–109. doi: 10.1161/01.RES.76.1.102

Stern, M. D., Maltseva, L. A., Juhaszova, M., Sollott, S. J., Lakatta, E. G., and Maltsev, V. A. (2014). Hierarchical clustering of ryanodine receptors enables emergence of a calcium clock in sinoatrial node cells. *J. Gen. Physiol.* 143, 577–604. doi: 10.1085/jgp.201311123

Tohse, N. (1990). Calcium-sensitive delayed rectifier potassium current in guinea pig ventricular cells. *Am. J. Physiol.* 258, H1200–H1207.

Trafford, A. W., Díaz, M. E., and Eisner, D. A. (2001). Coordinated control of cell Ca^{2+} loading and triggered release from the sarcoplasmic reticulum underlies the rapid inotropic response to increased L-type Ca^{2+} current. *Circ. Res.* 88, 195–201. doi: 10.1161/01.RES.88.2.195

Trafford, A. W., Díaz, M. E., Sibbring, G. C., and Eisner, D. A. (2000). Modulation of CICR has no maintained effect on systolic Ca^{2+}: simultaneous measurements of sarcoplasmic reticulum and sarcolemmal Ca^{2+} fluxes in rat ventricular myocytes. *J. Physiol.* 522, 259–270. doi: 10.1111/j.1469-7793.2000.t01-2-00259.x

van Borren, M. M. G. J., Verkerk, A. O., Wilders, R., Hajji, N., Zegers, J. G., Bourier, J., et al. (2010). Effects of muscarinic receptor stimulation on Ca^{2+} transient, cAMP production and pacemaker frequency of rabbit sinoatrial node cells. *Basic. Res. Cardiol.* 105, 73–87. doi: 10.1007/s00395-009-0048-9

van Borren, M. M. G. J., Zegers, J. G., Verkerk, A. O., and Wilders, R. (2007). Computational model of rabbit SA node pacemaker activity probed with action potential and calcium transient clamp. *Conf. Proc. IEEE Eng. Med. Biol. Soc.* 2007, 156–159. doi: 10.1109/IEMBS.2007.4352246

Varro, A., Negretti, N., Hester, S. B., and Eisner, D. A. (1993). An estimate of the calcium content of the sarcoplasmic reticulum in rat ventricular myocytes. *Pflügers Arch.* 423, 158–160. doi: 10.1007/BF00374975

Verheijck, E. E., van Ginneken, A. C. G., Wilders, R., and Bouman, L. N. (1999). Contribution of L-type Ca^{2+} current to electrical activity in sinoatrial nodal myocytes of rabbits. *Am. J. Physiol.* 276, H1064–H1077.

Verkerk, A. O., Baartscheer, A., de Groot, J. R., Wilders, R., and Coronel, R. (2011). Etiology-dependency of ionic remodeling in cardiomyopathic rabbits. *Int. J. Cardiol.* 148, 154–160. doi: 10.1016/j.ijcard.2009.10.047

Verkerk, A. O., den Ruijter, H. M., Bourier, J., Boukens, B. J., Brouwer, I. A., Wilders, R., et al. (2009). Dietary fish oil reduces pacemaker current and heart rate in rabbit. *Heart Rhythm* 6, 1485–1492. doi: 10.1016/j.hrthm.2009.07.024

Verkerk, A. O., van Borren, M. M. G. J., and Wilders, R. (2013). Calcium transient and sodium-calcium exchange current in human versus rabbit sinoatrial

node pacemaker cells. *ScientificWorldJournal* 2013:507872. doi: 10.1155/2013/507872

Verkerk, A. O., and Wilders, R. (2010). Relative importance of funny current in human versus rabbit sinoatrial node. *J. Mol. Cell. Cardiol.* 48, 799–801. doi: 10.1016/j.yjmcc.2009.09.020

Verkerk, A. O., Wilders, R., Coronel, R., Ravesloot, J. H., and Verheijck, E. E. (2003). Ionic remodeling of sinoatrial node cells by heart failure. *Circulation* 108, 760–766. doi: 10.1161/01.CIR.0000083719.51661.B9

Verkerk, A. O., Wilders, R., Zegers, J. G., van Borren, M. M. G. J., Ravesloot, J. H., and Verheijck, E. E. (2002). Ca^{2+}-activated Cl$^-$ current in rabbit sinoatrial node cells. *J. Physiol.* 540, 105–117. doi: 10.1113/jphysiol.2001.013184

Vermeulen, J. T., McGuire, M. A., Opthof, T., Coronel, R., de Bakker, J. M. T., Klöpping, C., et al. (1994). Triggered activity and automaticity in ventricular trabeculae of failing human and rabbit hearts. *Cardiovasc. Res.* 28, 1547–1554. doi: 10.1113/jphysiol.2001.013184

Vinogradova, T. M., Bogdanov, K. Y., and Lakatta, E. G. (2002a). β-adrenergic stimulation modulates ryanodine receptor Ca^{2+} release during diastolic depolarization to accelerate pacemaker activity in rabbit sinoatrial nodal cells. *Circ. Res.* 90, 73–79. doi: 10.1161/hh0102.102271

Vinogradova, T. M., Bogdanov, K. Y., and Lakatta, E. G. (2002b). Novel perspectives on the beating rate of the heart. *Circ. Res.* 91:e3. doi: 10.1161/01.RES.0000031164.28289.55

Weber, C. R., Piacentino, V. III, Houser, S. R., and Bers, D. M. (2003). Dynamic regulation of sodium/calcium exchange function in human heart failure. *Circulation* 108, 2224–2249. doi: 10.1161/01.CIR.0000095274.72486.94

Wiegerinck, R. F., Verkerk, A. O., Belterman, C. N., van Veen, T. A. B., Baartscheer, A., Opthof, T., et al. (2006). Larger cell size in rabbits with heart failure increases myocardial conduction velocity and QRS duration. *Circulation* 113, 806–813. doi: 10.1161/CIRCULATIONAHA.105.565804

Witte, K., Hu, K., Swiatek, J., Müssig, C., Ertl, G., and Lemmer, B. (2000). Experimental heart failure in rats: effects on cardiovascular circadian rhythms and on myocardial β-adrenergic signaling. *Cardiovasc. Res.* 47, 350–358. doi: 10.1016/S0008-6363(00)00099-7

Wu, Y., and Anderson, M. E. (2014). CaMKII in sinoatrial node physiology and dysfunction. *Front. Pharmacol.* 5:48. doi: 10.3389/fphar.2014.00048

Zicha, S., Fernandez-Velasco, M., Lonardo, G., L'Heureux, N., and Nattel, S. (2005). Sinus node dysfunction and hyperpolarization-activated (HCN) channel subunit remodeling in a canine heart failure model. *Cardiovasc. Res.* 66, 472–481. doi: 10.1016/j.cardiores.2005.02.011